JOURNAL OF GEOPHYSICAL RESEARCH, VOL. 105, NO. B11, PAGES 25,513–25,524, NOVEMBER 10, 2000

Hydrodynamic response to strike- and dip-slip faulting in a half-space

Shemin Ge and S. Chereé Stover

Department of Geological Sciences, University of Colorado, Boulder

Abstract. Field observations have shown strong coupling between earthquake-induced stress-strain fields and subsurface hydrodynamics, reflected by water level change in wells and stream flow fluctuations. Various models have been used in an attempt to interpret the coseismic fluctuations in groundwater level, predict water table rise in the event of an earthquake, and explain stream flow variations. However, a general model integrating earthquake-induced stress-strain fields, coseismic pore pressure generation, and postseismic pore pressure diffusion is still lacking. This paper presents such a general framework with which one can approach the general problem of postseismic pore pressure diffusion in three dimensions. We first use an earthquake strain model to generate the stress-strain field. We then discuss the linkage coupling stress and strain with pore pressure and present an analytical solution of time-dependent pore pressure diffusion. Finally, we use two examples, a strike-slip and a dip-slip fault, to demonstrate the application of the analytical model and the effects of earthquakes on fluid flow. The application to the two fault systems shows that the diffusion time is shorter than conventional estimates, which are based on a diffusivity and a length scale. We find that the diffusion time is predominately a function of the diffusivity of the system, while the length scale influences the magnitude of the initial pore pressure. A diffusion time based on the diffusivity and a length may be misleading because significant localized flow occurs in complex three-dimensional systems. Furthermore, the induced patterns of a pore pressure change resemble the strain field when shear stress effects are neglected but are significantly modified when shear stresses are included in the coupling relation. The theoretical basis of this work is developed assuming a single episode dislocation. However, the methodology and the results can be readily applied to studying pore pressure conditions after multifaulting events by simple superposition.

1. Introduction

Field observations have shown strong coupling between earthquake-induced stress-strain fields and subsurface hydrodynamics, as reflected in water levels in wells [e.g., *Roeloffs*, 1996] and stream flow fluctuations [*Rojstaczer and Wolf*, 1992, *Muir-Wood and King*, 1993]. Water level fluctuations as large as 90 cm in Nevada [*O'Brien*, 1992] and up to 5 m [*Roeloffs et al.*, 1995] were recorded in wells after the Landers earthquake in California in 1992. The release of the elastic strain energy in rocks during an earthquake causes rock compression or expansion, thereby redistributing the stress and strain in rocks. Consequently, pore pressure in the suddenly stressed regime is disturbed, either increasing or decreasing in response to compressional or extensional stresses. It is the disturbed pore pressure field that causes coseismic hydrologic responses and drives postseismic pressure diffusion. Two types of hydrologic responses caused by the quasi-static coseismic strain and the dynamic strain due to seismic waves manifest in reaction to earthquakes. The coseismic strain produces water level rise or fall, which is observed in the vicinity of an earthquake focus where the significant strain change occurs in the porous media. The dynamic strains due to seismic waves damp out rapidly compared to the time scale of pore pressure diffusion, and no permanent strains are expected after the waves pass. This paper focuses on hydrodynamic response caused by the quasi-static coseismic strain.

Paper number 2000JB900233.
0148-0227/00/2000JB900233$09.00

The basic physics describing earthquake-induced hydrologic response comprises three components: seismically-induced mechanical deformation, pore pressure diffusion, and coupling of the two. Classic elasticity [*Jaeger and Cook*, 1976] is generally the basis used by researchers studying deformation, while the well-known diffusion theory [*Carslaw and Jaeger*, 1959] serves as the basis for studying pore pressure dynamics. To fully understand the coupled phenomena from a theoretical standpoint, one needs to consider the impact of mechanical deformation on pore pressure diffusion and the influence of pore pressure on mechanical deformation. *Terzaghi*'s [1923] theory on soil consolidation may be regarded as one of the earliest contributions to the hydromechanical coupling problem. The benchmark papers by *Biot* [1941, 1955] presented a set of fully coupled deformation and pressure diffusion equations. Further, Biot provided analytical solutions of displacement and pore pressure as functions of time under a sudden loading in a one-dimensional domain.

Efforts toward understanding the coupling between deformation and induced pore pressure have been enhanced by many researchers in the past half century. For example, *Rice and Cleary* [1976] developed solutions for deformation

in saturated and compressible porous media. Furthermore, measurement of drained and undrained poroelastic parameters [e.g., *Green and Wang*, 1986] has greatly enhanced the study of coupled phenomena. A comprehensive evaluation of this subject is beyond the intention of this paper, and interested readers are encouraged to pursue excellent reviews by *Roeloffs* [1996] and *Wang* [2000]. However, it is important to make two relevant observations concerning deformation coupled with pore pressure. First, fully coupling deformation and pore pressure in three dimensions is often mathematically formidable, although numerical modeling approaches have been undertaken for basin-scale applications [e.g., *Ge and Garven*, 1992, 1994]. Second, two different timescales are involved, as recognized by *Palciauskas and Domenico* [1989]. Under earthquake conditions they are the short coseismic timescale, which is of the order of seconds, and the long pressure diffusion timescale, which is of the order of days to years.

In light of the abovementioned observations, a practical approach to coupled hydromechanical problems has been to decouple the deformation from pore pressure generation and diffusion and to use a pore pressure and strain or stress relationship to bridge the two. A well-known relationship was pioneered by *Skempton* [1954], who used a coefficient that directly relates the normal stresses to pore pressure. A more recent advance on the coupling mechanism incorporates the effect of shear strain in the generation of pore pressure [*Wang*, 1997].

Efforts have been made to interpret coseismic fluctuations in groundwater level [e.g., *Rudnicki et al.*, 1993; *Quilty and Roeloffs*, 1997], predict water table rise in the event of an earthquake [*e.g., Carrigan et al.*, 1991], and explain observed stream flow variations [e.g., *Rojstaczer and Wolf*, 1992; *Muir-Wood and King*, 1993]. Various models have been used in these endeavors, and yet a generic model integrating earthquake-induced stress-strain fields, coseismic pore pressure generation, and postseismic pore pressure diffusion under different faulting scenarios is still lacking. The purpose of this paper is to present such a generic framework. First, we use an earthquake strain model [*Okada*, 1992] to generate the three-dimensional stress-strain field. We then discuss the linkage coupling stress-strain to pore pressure and present an analytical solution of pore pressure diffusion in three dimensions. Finally, we use two examples, a strike-slip and a dip-slip fault, to demonstrate the effects of earthquake strains on fluid flow.

We recognize that this study is a simple first-order model that demonstrates the physics of the system. However, we hope that the results of this study will provide a means with which to evaluate hydrologic conditions after an earthquake on both spatial and temporal scales. It has been suggested that postseismic pore pressure plays a role in aftershocks [*Nur and Booker*, 1972] and in postseismic rebound [*Peltzer et al.*, 1996]. A better understanding of the hydrology may aid in revealing additional information useful for aftershock prediction.

2. Coseismic Strain Field

The spatial distribution of stress and strain around a fault has been a subject pursued by researchers for decades [e.g., *Anderson*, 1951]. Approaches range from theoretical treatment of displacement and stress distribution [e.g., *Pollard and Segall*, 1987] to numerical simulation using the boundary element method [e.g., *Bilham and King*, 1989]. We do not intend to provide a comprehensive literature review in this paper, but several relevant aspects should be presented. First, linear elasticity has been the dominant theoretical basis for most of these studies. The crust to first order behaves elastically on short timescales [e.g., *King et al.*, 1988]. Inelastic behavior [*Rundle*, 1982] tends to occur over longer timescales or in narrow fault zones. Second, the dislocation method, specifying the fault slip as dislocation along certain boundaries, has been widely employed to obtain stress-strain distributions. Studies have progressed from an idealized infinite fault plane to more realistic faults with finite dimensions [*Okada*, 1992]. Third, only after the analytical solutions for handling a finite fault plane become available can stress-strain distributions be studied in three dimensions. In a comprehensive paper that represents the present state of the art, Okada [1992] developed a set of closed-form expressions for the internal displacement and strain due to shear and tensile faults in a half-space. Okada's solutions evolved from early works on displacement and stress fields in a half-space due to a point source [*Mindlin*, 1936; *Press*, 1965] and strike-slip faulting [*Chinnery*, 1961, 1963]. The theoretical basis of these solutions is to use Green's function to obtain the displacement field due to a dislocation in an elastic half-space with a stress free ground surface. In this study, strain distributions computed from Okada's displacement solutions are used as a starting point for subsequent study of pore pressure generation and dissipation.

3. Pore Pressure Diffusion

Fluid flow in saturated porous media is governed by a diffusion process. On the basis of mass conservation in porous media the diffusion equation in terms of pore pressure under homogeneous and isotropic conditions is given by [e.g., *Freeze and Cherry*, 1979; *Domenico and Schwartz*, 1998]:

$$\frac{\partial^2 P}{\partial x^2}+\frac{\partial^2 P}{\partial y^2}+\frac{\partial^2 P}{\partial z^2}=\frac{1}{D}\frac{\partial P}{\partial t} \tag{1a}$$

$$D=\frac{K}{S_s}\ , \tag{1b}$$

where P is the pore pressure; D is the hydraulic diffusivity related to K, the hydraulic conductivity, and S_s, the specific storage; x, y, and z are the spatial coordinates; and t is the temporal coordinate. Under specified boundary and initial conditions in terms of pore pressure or pressure gradient, (1a) can be solved for a pressure field as a function of time and space.

When the hydraulic condition of a region is disturbed by an earthquake strain field, the volumetric strain exerts a sudden stress on surrounding porous media. Pore pressures will increase or decrease in accordance with the compression or expansion nature of the earthquake strain field. If we consider this pore pressure disturbance as an initial condition, then a half-space solution to the pore pressure diffusion is analogous to a heat conduction solution provided by *Carslaw and Jaeger* [1959, p. 277]:

$$P(x,y,z,t)=\frac{1}{8(\pi D t)^{\frac{3}{2}}}\int_{-\infty}^{\infty}\int_{-\infty}^{\infty}\int_{-\infty}^{\infty} f(x',y',z')$$

$$\left(e^{-\frac{R^2}{4Dt}} - e^{-\frac{R'^2}{4Dt}} \right) dx'dy'dz', \quad (2)$$

where $R^2 = (x-x')^2 + (y-y')^2 + (z-z')^2$;
$R'^2 = (x-x')^2 + (y-y')^2 + (z+z')^2$; and $f(x', y', z')$ is the initial or coseismic pressure distribution. The magnitude of the initial pressure change will be discussed in section 4. The physical meaning of solution (2) is that the pore pressure at any point in time, $P(x, y, z, t)$, will be a result of the initial disturbance field, $f(x',y',z')$, and diffusion of these disturbances with time t. It should be noted that solution (2) is the theoretical response of the pore pressure to a sudden strain change under idealized homogeneous and isotropic conditions. Real geologic media may well be heterogeneous, and earthquake events are episodic. However, since (1a) is linear, it is possible to apply solution (2) to episodic earthquake events, using the superposition principle. For example, in the case of a major earthquake followed by a series of aftershocks, one can repeatedly use solution (2) to obtain a resultant pore pressure field. Therefore, although the pressure diffusion conceptualized in this study is developed for a generic single episode scenario, it provides a useful means for further study on the hydrologic response of porous medium under more complex seismic-loading conditions.

4. Coupling Coseismic Strain and Pore Pressure Change

While elastic deformation and pore pressure diffusion are well-established theories, the coupling between the mechanical stress-strain field and the induced pore pressure has continued evolving since the conception of *Terzaghi*'s [1923] soil consolidation theory. To fully couple the mechanics and hydrology, one needs to modify elasticity theory to represent poroelasticity [*Mandl*, 1988; *Wang*, 2000] by including a pore pressure term in the force equilibrium equation and using poroelastic constants instead of pure elastic constants. Similarly, (1a), describing pressure diffusion, needs to be modified to include a stress or strain term. Pioneering the fully coupled problem, *Biot* [1941, 1955] provided a set of three-dimensional equations and solved the one-dimensional consolidation problem in a soil column. *Rudnicki* [1987] solved for two-dimensional coupled stress and pore pressure with a dislocation along a semi-infinite surface. Mathematically solving the fully coupled problem in three dimensions would be an unrealistic mathematical endeavor, but an alternate approach has proven to be practical. Such an approach decouples mechanical deformation from the pressure diffusion equations, but uses a linkage to relate the strain and pressure change, as discussed below.

To examine the hydrodynamic processes closely, we first identify two timescales, coseismic and postseismic. The coseismic timescale is often short, of the order of seconds. The postseismic scale, associated with the pressure diffusion process, is several orders of magnitude longer, ranging from hours to years, depending mainly on the hydraulic diffusivity of the porous medium under consideration. The difference between these two timescales effectively allows the decoupled approach to be applicable. It is reasonable to assume that the coseismic pressure change is instantaneous

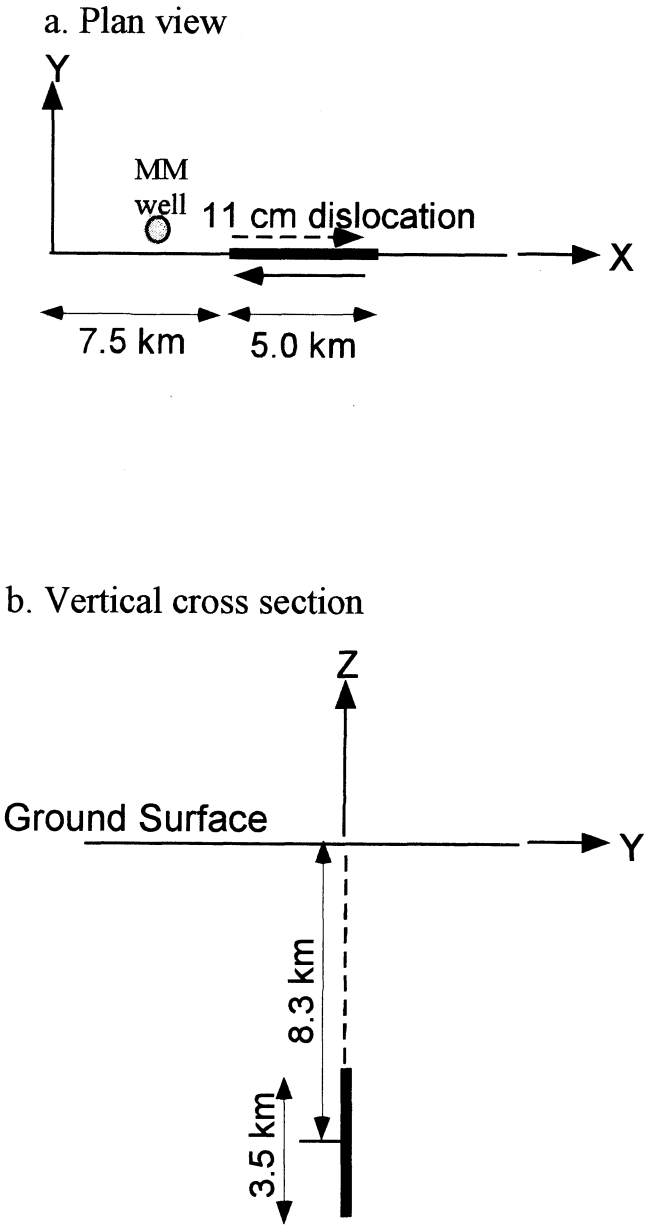

Figure 1. A right-lateral strike-slip fault geometry. Geometric specifications are taken from *Quilty and Roeloffs* [1997]. The thick black line indicates the fault trace. The shaded circle is the Middle Mountain monitoring well.

and that the postseismic dissipation of pore pressure takes place over a much longer period as described by (2).

The relationships between the change in the stress-strain field and the induced pressure change have been derived from various avenues. *Biot*'s [1941, 1955] early work gave the following expression for pore pressure change, ΔP [e.g., *Green and Wang*, 1986]:

$$\Delta P = -\frac{B}{3}\Delta\sigma_{ii}, \quad (3)$$

where B is the experimentally determined *Skempton* [1954] coefficient and $\Delta\sigma_{ii}$ are the changes in principal stresses. The sign convention is such that positive stress represents tension, while negative stress represents compression. As such,

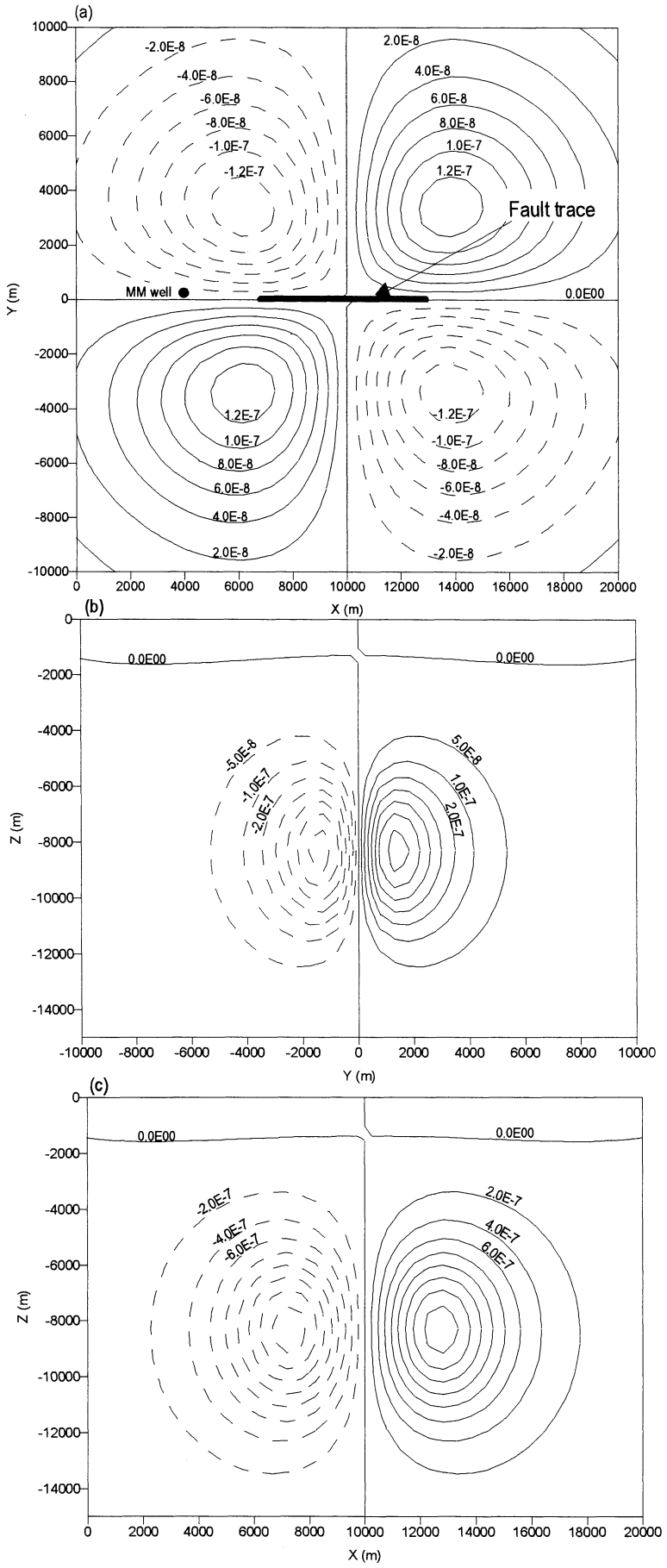

Figure 2. Volumetric strain distribution due to a right-lateral strike-slip dislocation of 11 cm. The solid lines represent expansion, and the dashed lines represent compression.

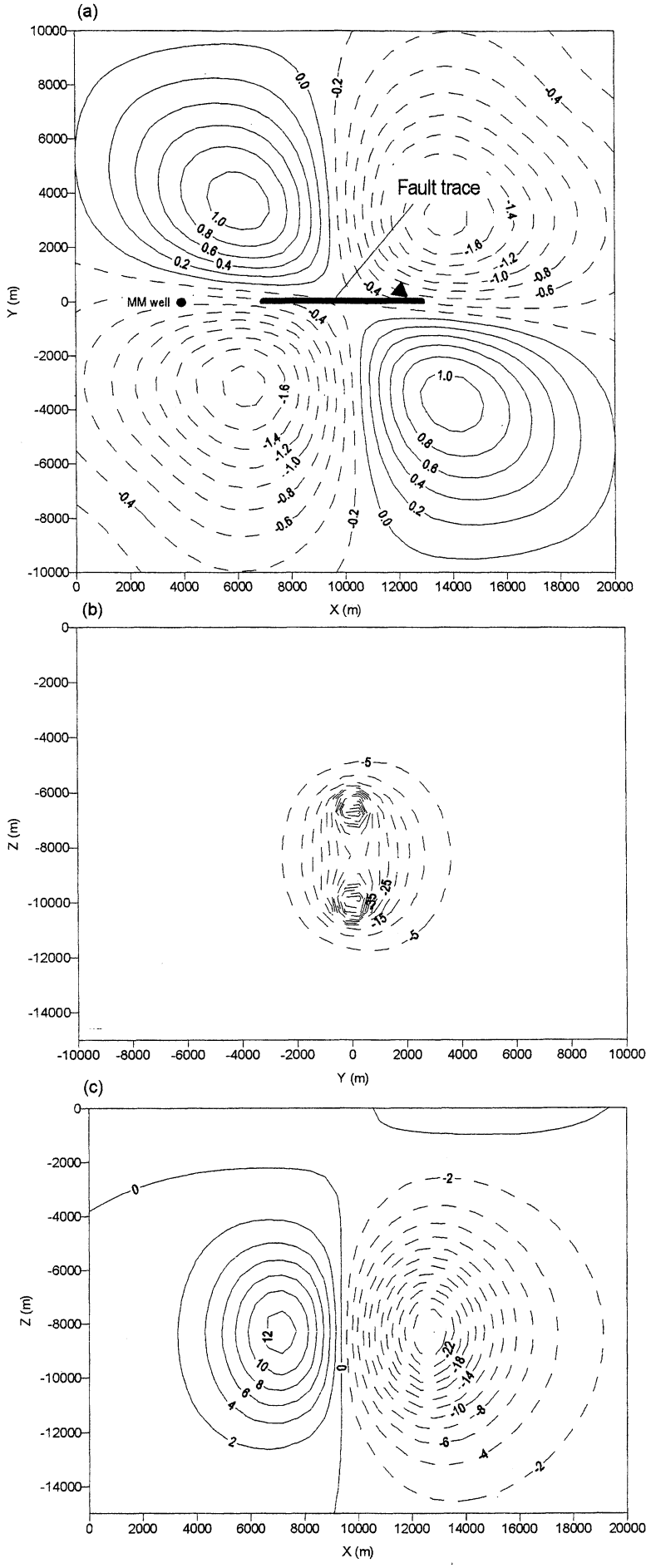

Figure 3. Water level change (in meters) corresponding to the three locations where the volumetric strains are depicted in Figure 2. The solid lines represent water level increase, and the dashed lines represent water level decrease.

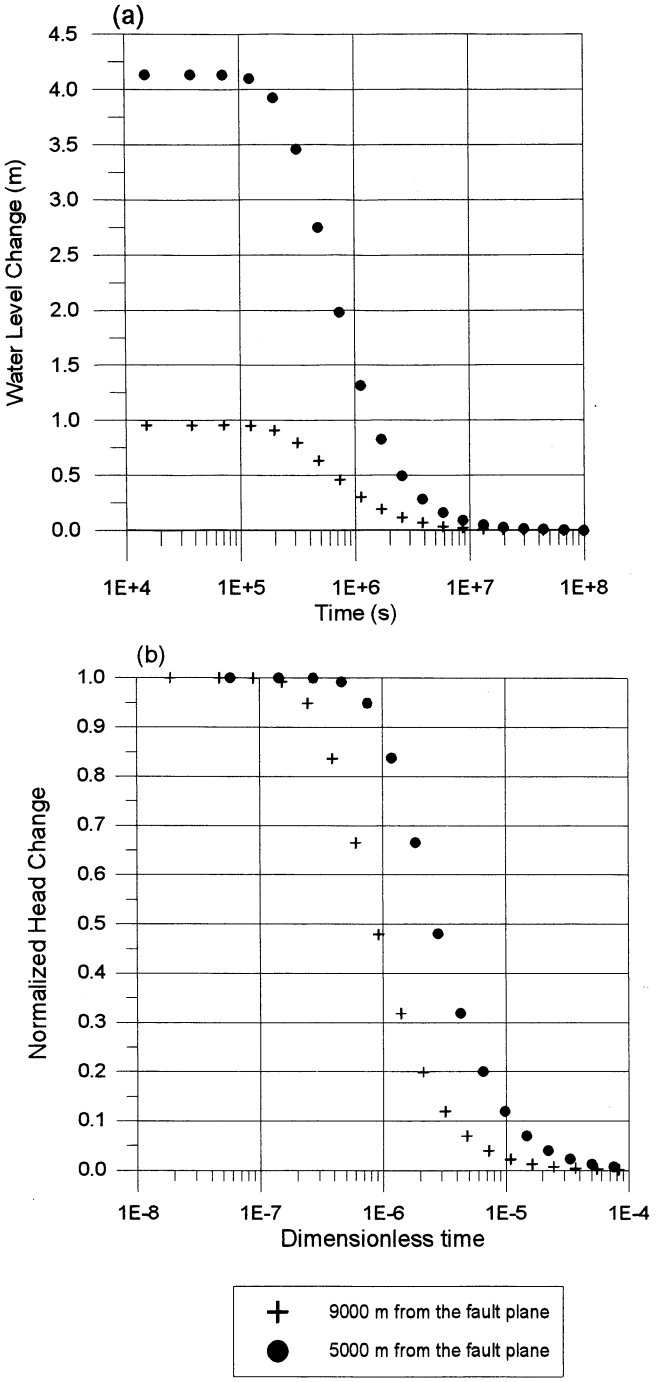

Figure 4. Water level change as a function of time at two observation points for the strike-slip fault case. The dots represent the point at x = 6750 m, y = 2250 m, and z = -250 m, or 5000 m from the center of the fault plane and the crosses represent the point at x = 14250 m, y = 1250 m, and z = -5750 m, or 9000 m from the fault center. Hydraulic diffusivity D is 0.0001 m^2/s. (a) The water level change versus time in actual units. (b) Dimensionalized by the maximum water level change at that same location and by a characteristic time L^2/D, where L is the distance from the observation point to the geometric center of the fault plane.

positive pore pressure change relates to water level rise, and negative pore pressure change relates to water level fall. Relation (3) assumes that shear stress does not produce volumetric strain or influence pore pressure and thus only relates normal stresses to pore pressure. This notion has been contested by subsequent experimental and theoretical contributions which include the effect of shear stress on induced pore pressure change [*Skempton*, 1954; *Henkel*, 1960; *Henkel and Wade*, 1966; *Wang*, 1997],

$$\Delta P = -B\left[\frac{1}{3}\Delta\sigma_{ii} + \frac{3A-1}{\sqrt{2}}\Delta\tau^{oct}\right], \tag{4}$$

where both A and B are experimentally determined coefficients and τ^{oct} is the octahedral shear stress invariant defined by [*Jaeger and Cook*, 1976, p. 24]:

$$\tau^{oct} = \frac{1}{3}\left[(\sigma_{11}-\sigma_{22})^2 + (\sigma_{22}-\sigma_{33})^2 (\sigma_{33}-\sigma_{11})^2\right]^{\frac{1}{2}}. \tag{5}$$

In addition to (3) and (4), various forms of equations have been used to relate pore pressure change to stress or strain [e.g., *Bredehoeft*, 1967; *Rice and Cleary*, 1976; *van der Kamp and Gale*, 1983], all of which identify a simple linear relationship between the change in pore pressure and volumetric strain change:

$$\Delta P = C\Delta\theta, \tag{6}$$

where the proportionality C is a function of porous medium properties such as bulk compressibility and $\Delta\theta$ is the volumetric strain change. Upon determining the stress or strain field, we can use one of the coupling relations, (4) or (6), to determine ΔP as the initial condition, $f(x', y', z')$, and then compute the pore pressure, $P(x, y, z, t)$, from solution (2).

When the stress state is known, (4) can be used to find the pressure change due to changes in both normal stress and shear stress. However, (6) is preferred when the strain field is measured or is a known quantity. The two equations can be unified by considering the constitutive relation between stress and strain as outlined below. The constitutive relation for a poroelastic medium is similar to that for an elastic medium except that the parameters in the poroelastic case are undrained parameters:

$$2G_u\Delta\varepsilon_{ij} = \Delta\sigma_{ij} - \frac{\gamma_u}{1+\gamma_u}\Delta\sigma_{kk}\delta_{ij}, \tag{7}$$

where G_u is the undrained shear modulus, ε_{ij} is the strain tensor, γ_u is the undrained Poisson's ratio, and δ_{ij} is the Kronecker delta. Adding (7) gives the volumetric strain:

$$\Delta\theta = \Delta\varepsilon_{ii} = \frac{1-2\gamma_u}{E}\Delta\sigma_{ii} \quad \text{or} \quad \Delta\sigma_{ii} = \frac{E}{1-2\gamma_u}\Delta\theta, \tag{8}$$

where E is the Young's modulus. If we ignore the octahedral shear stress in (4) for now and compare (4), (6), and (8), we can establish the equivalency between (4) and (6) by the following:

$$C = -BG_u\frac{2(1-\gamma_u)}{3(1-2\gamma_u)}. \tag{9}$$

When B = 1, C becomes the undrained bulk modulus. Our current understanding on the relationship between shear stress and induced pore pressure is only at the experimentally observed level. Future theoretical development could lead to a modified constitutive relation that may add a shear stress term in (7).

5. Application

5.1. Strike-Slip Fault

Given the theoretical framework discussed above, we present two cases of earthquake-induced hydrodynamic

response. The first case illustrates hydrodynamic response to strike-slip faulting. A magnitude 4.7 earthquake near Parkfield, California, on December 20, 1994, is used. As shown in Figure 1, the earthquake was a result of a right-lateral strike-slip fault which ruptured at a depth of 8.3 km over a 5.0 km × 3.5 km fault plane with an 11 cm dislocation [*Quilty and Roeloffs*, 1997].

Using the solution obtained by *Okada* [1992], we computed the three-dimensional coseismic strain field due to the 11 cm dislocation on the vertical fault plane. The center of the fault plane is at x = 10000 m, y = 0, and z = - 8300 m. For an undrained Poisson's ratio of 0.3, the three-dimensional volumetric strain field is shown in three cross sections in Figure 2. Figure 2a presents the volumetric strain in plane view at a depth of 250 m below the surface, and Figures 2b and 2c are two cross-sectional views of the volumetric strain field at x = 9750 m and y = -2750 m, respectively. The solid lines represent regions of expansion, and the dashed lines represent compression. The four-quadrant pattern (Figure 2a) is what we expect from a strike-slip dislocation source. However, it is interesting to note that the sign of the volumetric strain in Figure 2a is somewhat counterintuitive, while the signs at depth (Figures 2b and 2c) are as expected. For example, the upper right quadrant in Figure 2a is under tension rather than compression. This is due to the fact that the dislocating fault plane has a finite vertical dimension and it is buried below the surface. The expected compression near the tip of the fault leads to expansion farther away in order to satisfy the free stress boundary condition at the surface and force equilibrium. As shown in Figures 2b and 2c, the signs of the strain reverse as they approach the surface.

For a given shear modulus G_u and undrained Poisson's ratio γ_u the stresses can be computed from the strain field using equation (7). We used $G_u = 5 \times 10^{10}$ Pa and $\gamma_u = 0.3$ [*Roeloffs*, 1996]. A recent study by *Wang* [1997] found that including the shear stress was necessary to explain the pore pressure increase near the strike-slip fault. We used (4) to compute the pore pressure change and converted the pressure change to a head change by $\Delta h = \Delta P/\rho g$, where ρ is the density of water and g is the gravitational acceleration. This conversion is of interest since the head change at perforated depths in wells could be a direct estimate of water level change in the well. The two experimental coefficients, A and B, in equation (4) are given the values of 0.2 and 1, respectively [*Wang*, 1997]. Shown in Figure 3 are the head or water level changes in three cross sections corresponding to the volumetric strain cross sections presented in Figure 2. The solid lines represent water level increase and dashed lines represent water level drop. Two observations can be made. First, it is important to note that the variation in the vertical direction implies that the response of water levels in wells perforated at different depths may vary significantly. Second, the coseismic water level change is constrained spatially by the volumetric strain field. The asymmetry of the water level change pattern shown in Figure 3a is due to the inclusion of shear-stress effects [*Wang*, 1997], particularly in the vicinity of the fault where shear is a significant deformation mode. If we neglect the effect of shear stress, water level change patterns will mimic the symmetric patterns of strain. Including the shear stress effects, relation (4) has helped to explain the coseismic rise and fall patterns of the water level near the fault trace associated with the Parkfield, December

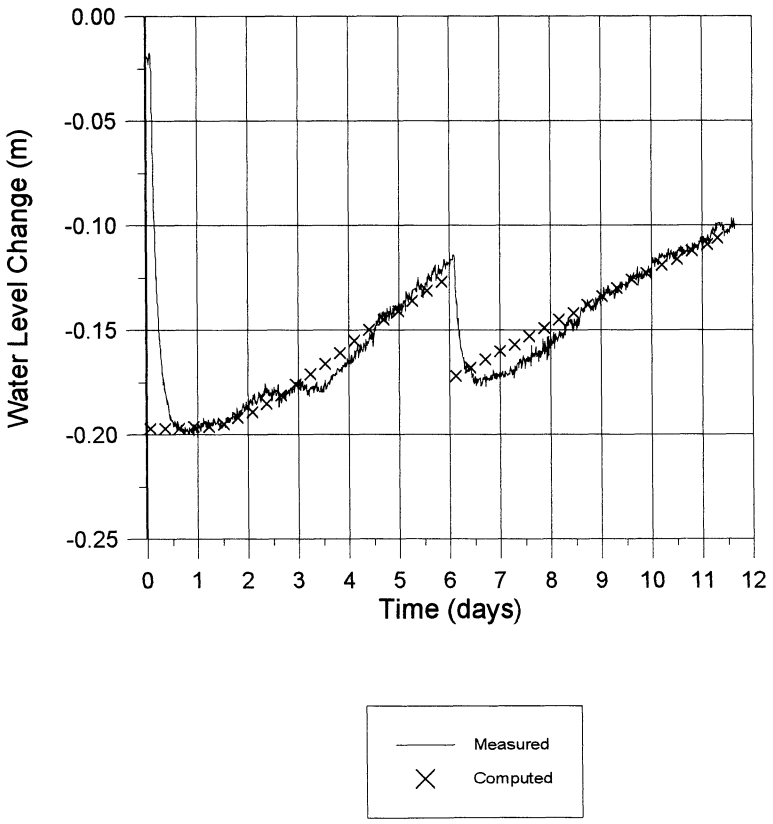

Figure 5. Comparison of measured and computed water level recovery data in the Middle Mountain well after the Parkfield, December 20, 1994, earthquake.

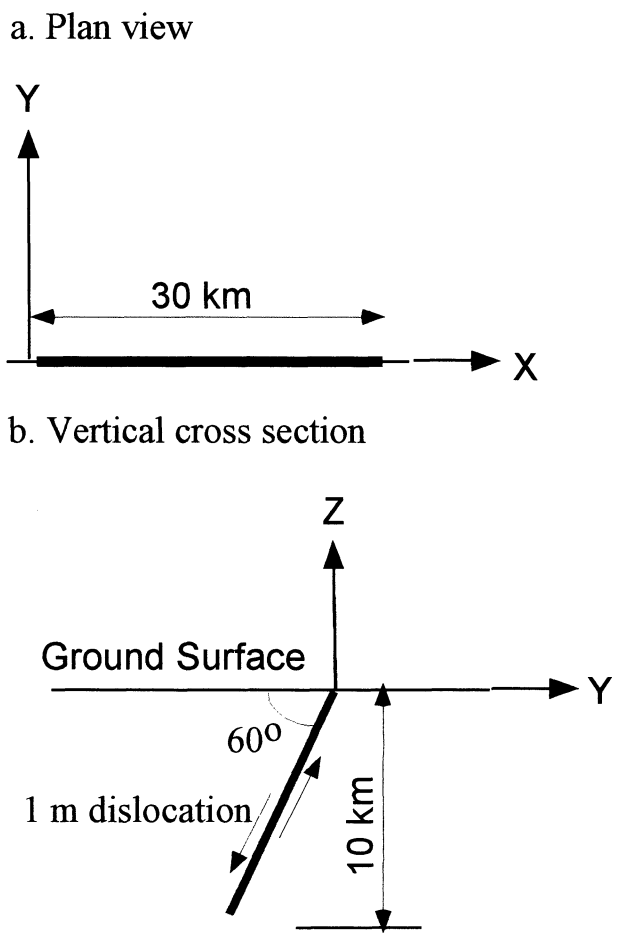

Figure 6. A dip-slip fault system. The geometric specifications are taken from *Bredehoeft* [1992]. The thick black line indicates the fault trace.

20, 1994, earthquake, which otherwise could not be explained by a normal stress model [*Wang*, 1997; *Quilty and Roeloffs*, 1997].

To illustrate the long-term postseismic pressure diffusion process, given the conditions of the Parkfield earthquake, we used solution (2) to calculate the pressure as a function of time at two observation points. The first point is located at x = 6750 m, y = 2250 m, and z = -250 m, or 5000 m from the center of the fault plane, and the second point is farther away, at x = 14250 m, y = 1250 m, and z = -5750 m, or 9000 m from the fault center. Figure 4 shows the postseismic diffusion of the pressure in terms of water level at these two locations for a diffusivity of 10^{-4} m^2/s. Several observations can be made. First, the diffusion time shown in Figure 4a is of the order of 10^6 s (~300 hours), which is much shorter than the commonly cited estimates in the existing hydrology literature. The diffusion time is an indicator of how fast disturbed water levels recover and is conventionally estimated by the following relation [e.g., *Carslaw and Jaeger*, 1959; *Nur and Booker*, 1972; *Phillips*, 1991, p. 82]:

$$t \approx \frac{L^2}{D}, \tag{10}$$

where L is a characteristic length, commonly taken as the distance between the source and the observation point or the dimension of the study domain, and D is the hydraulic diffusivity. For a single point source disturbance, (10) serves well as an estimate. In the case of a complex strain field, the dissipation of excess pore pressure at a given location is a result of contributions from the distributed strain in three dimensions. The shorter diffusion time found in this example appears to be due to the fact that significant localized flow occurs from over pressured to under pressured regions.

A second interpretation of the results in Figure 4 focuses on coseismic pore pressure change. A smaller magnitude of coseismic pressure change is observed at the point farther away from the fault plane, as shown by the crosses in Figure 4a, while the near-source location experiences a larger pressure change, as shown by the dots in Figure 4a. The duration of influence, however, is about the same regardless of the distance from the seismicity. Casting the same data set into the dimensionless form, as shown in Figure 4b, we observe similar diffusion behavior for all the points. The shift in curve location is a direct reflection of the distance from seismicity. This observation implies that for a given diffusivity the time needed to propagate to far distances is compensated by the fact that smaller pressure change at the far distance requires less dissipation time.

We compared our computed coseismic and postseismic water levels with the measured water level recovery data [*Quilty and Roeloffs*, 1997] from the Middle Mountain (MM) well in Parkfield (Figure 5). The well location is shown in Figure 1. The MM well is perforated between 235 m to 247 m below the surface [*Roeloffs et al.*, 1989]. We selected the MM well because it shows a clear recovery pattern. The water level drop near day 6 suggests a creep event [*Quilty and Roeloffs*, 1997]. Solution (2) is used twice to superimpose the seismic and creep events. Satisfactory agreement is achieved for the given parameters in this scenario. The comparison between computed and measured water level recovery serves several purposes. First, it shows that solution (2) can be used to predict postseismic pore pressure diffusion or water level recovery in wells. Second, matched water level magnitude provides an estimation of the coupling or mechanical parameters to which the magnitude is sensitive. Third, by matching the water level decay pattern the hydraulic diffusion parameter can be inferred since the pattern is primarily a function of hydraulic diffusivity. We note that the real geologic system will be more complex than what we discuss here, but the result of this study provides a baseline estimation of the quantities of interest. It is also important to recognize that this study is a first-order model showing the basic physical processes operating in the coupled strain and pore pressure system. It is unlikely that this model could be applied to match all the well data without extensive manipulation, such as superposition in both time and space. To match a large number of data would call for a numerical model that incorporates more complexities.

5.2. Dip-Slip Fault

The second application example demonstrates earthquake-induced hydrologic response to a normal fault system. As shown in Figure 6, the fault extends from the surface to a depth of 10 km with a dipping angle of 60° and a width of 30 km. The hypothetical geometry is taken from *Bredehoeft* [1992], who evaluated the effect of a dip-slip fault earthquake on the water table rise in Yucca Mountain, Nevada, using a finite difference numerical model.

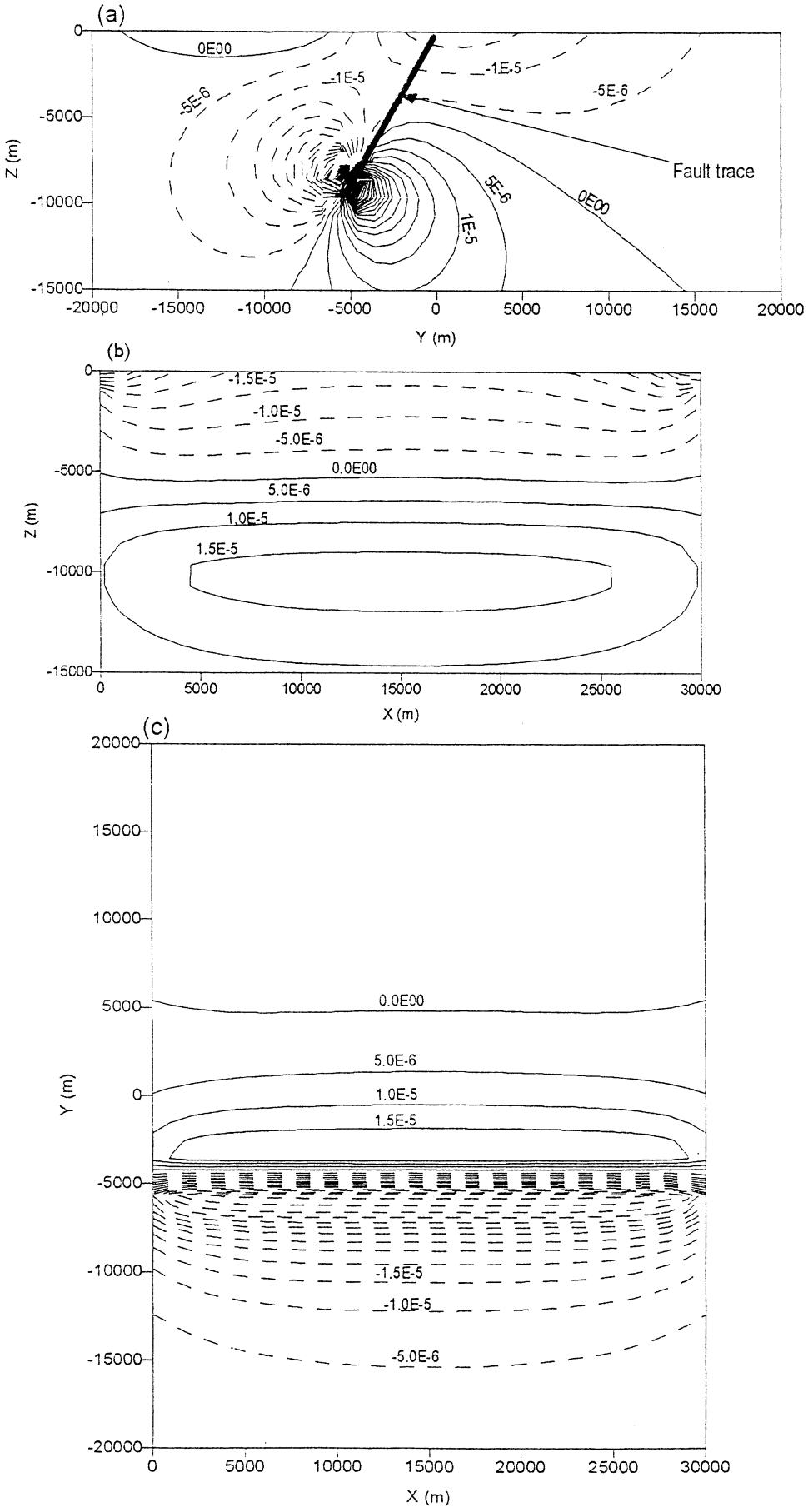

Figure 7. Volumetric strain distribution due to a normal displacement of 1 m. The solid lines represent expansion, and the dashed lines represent compression.

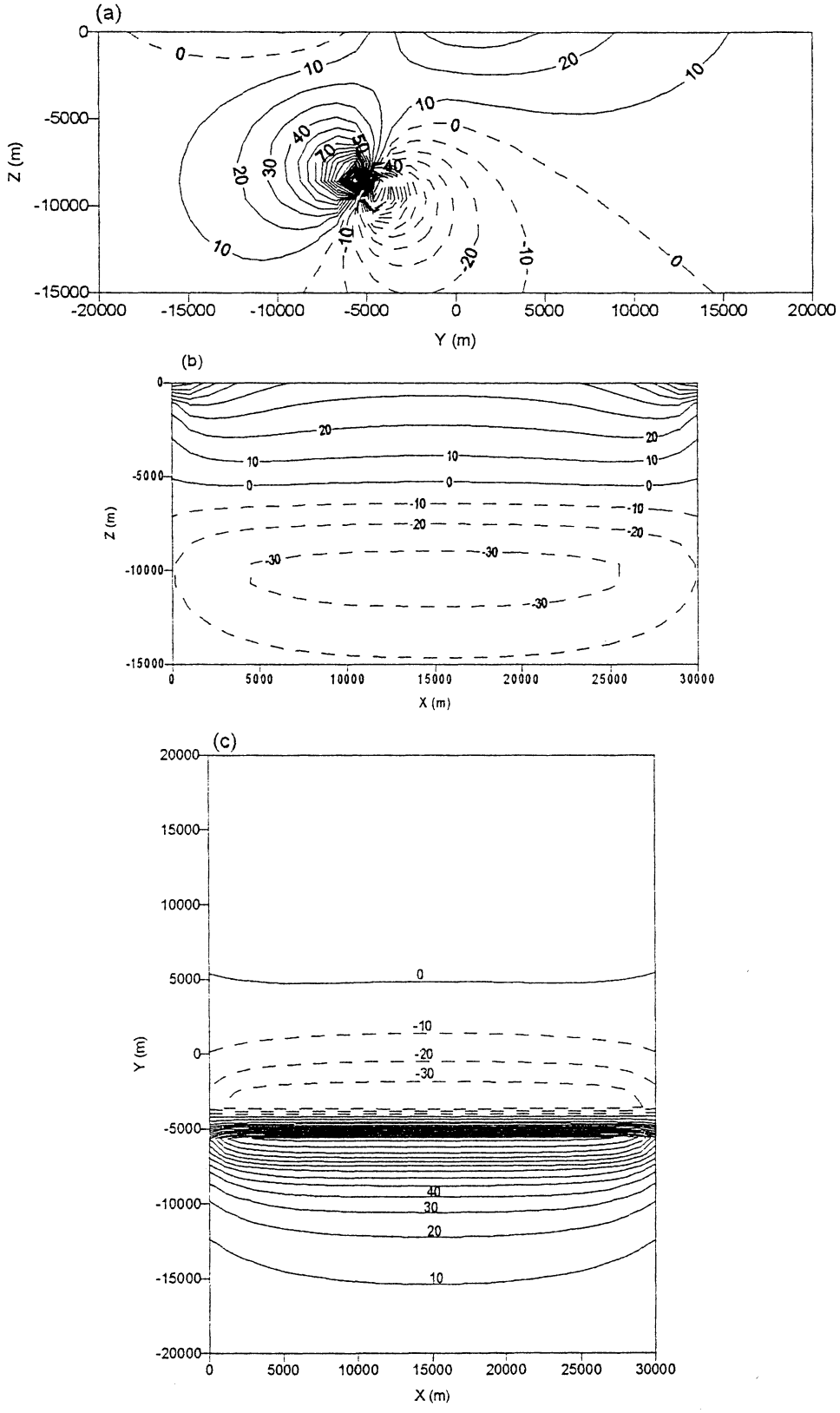

Figure 8. (a-c) Water level change (in meters) corresponding to the three locations where the volumetric strains are depicted in Figure 7. The solid lines represent water level increase, and the dashed lines represent water level decrease.

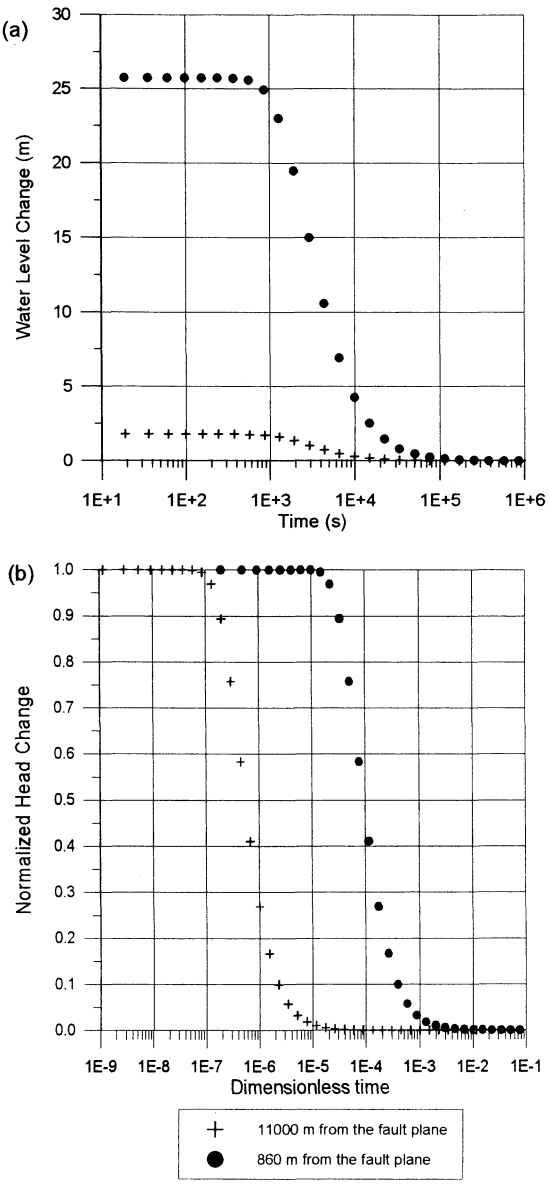

Figure 9. Water level change as a function of time at two observation points for the normal fault case. The dots represent the point at x = 14500 m, y = -5500 m, and z = -10500 m, or 860 m from the center of the fault plane and the crosses represent the point at x = 14500 m, y = -12500 m, and z = -150 m, or 11000 m from the fault center. Hydraulic diffusivity D is 0.01 m^2/s. (a) The water level change versus time in actual units. (b) Dimensionalized by the maximum water level change at the same location and by a characteristic time, L^2/D, where L is the distance from the observation point to the geometric center of the fault plane.

The domain considered is a homogeneous and isotropic block with a dimension of 30 km × 40 km × 15 km with the center of the fault plane located at x = 15000 m, y = 0, z = -5000 m. The undrained Poisson's ratio γ_u is assumed to be 0.3. Using the same *Okada* [1992] dislocation code as in the strike-slip faulting case, we computed the three-dimensional strain distribution in response to a 1 m dislocation of normal fault motion. The three-dimensional volumetric strain field is shown in Figure 7 with Figure 7a located at x = 14500 m, Figure 7b located at y = -500 m, and Figure 7c located at z = -7500 m. We used (6) to compute the coseismic pore pressure change, which simply relates the pore pressure to the volumetric strain by the bulk compressibility without considering the shear stress effect. Although (6) has the advantage of being simple and straightforward when the volumetric strain is known, the effect of shear stress on the pore pressure field is sacrificed. For this example, we would not expect the results to differ significantly if (4) were used. For a bulk compressibility ($1/C$) of 5 $\times 10^{-11}$ /Pa the water level changes are shown in three cross sections in Figure 8, corresponding to the same cross sections presented in Figure 7. When we compare Figures 7 and 8, it becomes apparent that the patterns of water level change closely resemble the volumetric strain distribution. Moreover, Figures 8a and 8b indicate that water levels vary with depth, thereby suggesting that fluctuation in the range of centimeters to tens of meters in wells at various depths can be expected in response to dip-slip faulting.

We also use solution (2) to calculate the pore pressure as a function of time at two observation points, one at x = 14500 m, y = -5500 m, and z = -10500 m, or 860 m from the center of the fault plane and the other at x = 14500 m, y = -12500 m, and z = -150 m, or 11000 m from the fault center. Figure 9 shows that the postseismic diffusion at these two locations exhibits similar patterns. The location farther from the fault plane has a smaller coseismic water level change, while the near-source location has a larger water level change. However, the duration of influence is on the same timescale regardless of the distance from the seismicity. The shift in dimensionalized curves in Figure 9b only reflects the differences in distance of the two points from the source.

6. Summary and Discussion

This study provides an integrated framework with which one can approach the general problem of postseismic pore pressure diffusion in three dimensions in response to dislocation of a finite fault plane. We use *Okada*'s [1992] solution to find the stress-strain field due to a dislocation on the finite fault plane. Pore pressure generation is computed using the stress-strain field and a relation that couples pore pressure and strain or stress. The generated pore pressure is then allowed to dissipate, governed by a diffusion process. Although the theoretical components of hydromechanical coupling have been well developed, this study integrates these components and implements an analytical solution for pore pressure diffusion that enables us to explore or predict coseismic and postseismic hydrologic behaviors. Our proposed generic model may also be useful for estimating hydrologic parameters, such as hydraulic diffusivity. It should be noted that this study is theoretical in nature and many of the real complexities are not incorporated. For example, faults are often found to be either impermeable barriers or permeable conduits, and hydraulic diffusivity can vary over orders of magnitude in heterogeneous media. We believe, however, that this study captures the basic essence of coupled deformation and fluid flow problems. Moreover, the basic model presented here can be applied to more complex systems through use of superpositions to study pore pressure conditions after multifaulting events, as illustrated in the strike-slip fault example.

We show the application of the model to a strike-slip and a dip-slip fault system. Our findings indicate that the actual diffusion time is shorter than conventional estimates based on a diffusivity and a length scale. We find that the diffusion time is predominately a function of diffusivity of the system.

The location or the length scale has a large influence on the magnitude of the initial head generation. A diffusion time based on a diffusivity and a length may give misleading results because significant localized flow occurs in complex three-dimensional systems. It is also important to understand that pressure at any point is a result of the initial pressure generated at that point, the diffusion process, and the influence of the initial pressure at other locations.

Acknowledgment. We are grateful to Eddie Quilty and Evelyn Roeloffs of the U.S. Geological Survey for providing the water level data of the MM well in Parkfield, California. We benefited from discussions with Herbert Wang of University of Wisconsin and Raymond Fletcher of University of Colorado. Special thanks go to Yoshimitsu Okada of Japan for allowing the authors to use his dislocation program. Reviews from Associate Editor Jeff Freymueller, Zheng-kang Shen, and an anonymous referee have greatly enhanced the mathematical rigorousness and overall quality of the paper. This study is supported in part by grants EAR-9804789 from the U.S. National Science Foundation and DEFG0395ER14518 from the U.S. Department of Energy.

References

Anderson, E.M., *The Dynamics of Faulting*, Oliver and Boyd, White Plains, N.Y., 1951.

Bilham, R., and G. King, The morphology of strike-slip faults: Examples from the San Andreas Fault, California, *J. Geophys. Res.*, *94*(B8), 10,204-10,216, 1989.

Biot, M.A., General theory of three-dimensional consolidation, *J. Appl. Phys.*, *12*, 155-164, 1941.

Biot, M.A., General solutions of the equations of elasticity and consolidation for a porous material, *J. Appl. Mech.*, *23*, 91-96, 1955.

Bredehoeft, J.D., Response of well-aquifer systems to Earth tides, *J. Geophys. Res.*, *72*(12), 3075-3087, 1967.

Bredehoeft, J.D., Response of the ground-water system at Yucca Mountain to an earthquake, in *Ground Water at Yucca Mountain, How High Can It Rise*?, 212-222, Nat. Acad. Press, Washington, D.C., 1992.

Carrigan, C.R., G.C.P. King, G.E. Barr, and N.E. Bixler, Potential for water-table excursions induced by seismic events at Yucca Mountain, Nevada, *Geology*, *19*, 1157-1160, 1991.

Carslaw, H.S., and J.C. Jaeger, *Conduction of Heat in Solids*, 510 pp., Oxford Univ. Press, New York, 1959.

Chinnery, M.A., The deformation of the ground around surface faults, *Bull. Seismol. Soc. Am.*, *51*(3), 355-372, 1961.

Chinnery, M.A., The stress changes that accompany strike-slip faulting, *Bull. Seismol. Soc. Am.*, *53*(5), 921-932, 1963.

Domenico, P.A., and F.W. Schwartz, *Physical and Chemical Hydrogeology*, 506 pp., John Wiley, New York, 1998.

Freeze, A.R., and J.A. Cherry, *Groundwater*, 604 pp., Prentice-Hall, Englewood Cliffs, N. J., 1979.

Ge, S., and G. Garven, Hydromechanical modeling of tectonically-driven groundwater flow with application to the Arkoma Foreland Basin, *J. Geophys. Res.*, *97*(B6), 9119-9144, 1992.

Ge, S., and G. Garven, A theoretical model for thrust-induced deep groundwater expulsion with application to the Canadian Rocky Mountains, *J. Geophys. Res.*, *99*(B7), 13,851-13,868, 1994.

Green, D.H., and H.F. Wang, Fluid pressure response to undrained compression in saturated sedimentary rock, *Geophysics*, *51*, 948-956, 1986.

Henkel, D.J., The shear strength of saturated remoulded clays, in *Proceedings of the American Society of Civil Engineers Research Conference on Shear Strength of Cohesive Soils*, pp. 533-554, Am. Soc. of Civ. Eng., New York, 1960.

Henkel, D.J., and N.H. Wade, Plane strain tests on a saturated remolded clay, *J. Soil Mech. Found. Div.*, *92*(SM6), 67-80, 1966.

Jaeger J.C., and N.G.W. Cook, *Fundamentals of Rock Mechanics*, 585 pp., John Wiley, New York, 1976.

King, G.C.P., R.S. Stein, and J.B. Rundle, The growth of geological structures by repeated earthquakes, 1, Conceptual framework, *J. Geophys. Res.*, *93*(B11), 13,307-13,318, 1988.

Mandl, G., *Mechanics of Tectonic Faulting: Models and Basic Concepts*, 407 pp., Elsevier Sci., New York, 1988.

Mindlin, R.D., Force at a point in the interior of a semi-infinite solid, *Physics*, *7*, 195-202, 1936.

Muir-Wood, R., and G.C.P. King, Hydrological signatures of earthquake strain, *J. Geophys. Res.*, *98*(B12), 22,035-22,068, 1993.

Nur, A., and J.R. Booker, Aftershocks caused by pore fluid flow?, *Science*, *175*, 885-887, 1972.

O'Brien, G.M., Earthquake-induced water-level fluctuations at Yucca Mountain, Nevada, June 1992, *U.S. Geol. Survey Open File Rep.*, *93-173*, 12 pp., 1992.

Okada, Y., Internal deformation due to shear and tensile faults in a half-space, *Bull. Seismol. Soc. Am.*, *82*(2), 1018-1040, 1992.

Palciauskas, V.V., and P.A. Domenico, Fluid pressure in deforming porous rocks, *Water Resour. Res.*, *25*, 203-219, 1989.

Peltzer, G., P. Rosen, F. Rogez, and K. Hudnut, Postseismic rebound in fault step-overs caused by pore fluid flow, *Science*, *273*, 1202-1204, 1996.

Phillips, O.M., *Flow and Reactions in Permeable Rocks*, 285 pp., Cambridge Univ. Press, New York, 1991.

Pollard, D.D., and P. Segall, Theoretical displacements and stresses near fractures in rock: with applications to faults joints, veins, dikes, and solution surfaces, in *Fracture Mechanics of Rock*, 277-349, Academic, San Diego, Calif., 1987.

Press, F., Displacements, strains, and tilts at teleseismic distances, *J. Geophys. Res.*, *70*(10), 2395-2412, 1965.

Quilty, E.G., and E.A. Roeloffs, Water-level changes in response to the 20 December 1994 earthquake near Parkfield, California, *Bull. Seismol. Soc. Am.*, *87*(2), 310-317, 1997.

Rice, J.R., and M.P. Cleary, Some basic stress diffusion solutions for fluid-saturated elastic porous media with compressible constituents, *Rev. Geophys.*, *14*(12), 227-241, 1976.

Rojstaczer, S., and S. Wolf, Permeability changes associated with large earthquakes: An example from Loma Prieta, California, *Geology*, *20*, 211-214, 1992.

Roeloffs, E.A., Poroelastic techniques in the study of earthquake-related hydrologic phenomena, *Adv. Geophys.*, *37*, 135-195, 1996.

Roeloffs, E.A., S.S. Burford, F.S. Riley, and A.W. Records, Hydrologic effects on water level changes associated with episodic fault creep near Parkfield, California, *J. Geophys. Res.*, *94* (B9), 12,387-12,402, 1989.

Roeloffs, E.A., W. Danskin, C. Farrar, D.L. Galloway, S. Hamlin, E.G. Quilty, H.M. Quinn, D.H. Schaefer, M. Sorey, and D. Woodcock, Hydrologic effects of the June 28, 1992, Landers, California, Earthquake, *U.S. Geol. Sur., Open File Rep., 95-42*, 1995.

Rudnicki, J.W., Plane strain dislocations in linear elastic diffusive solids, *J. Appl. Mech.*, *54*, 545-552, 1987.

Rudnicki, J.W., J. Yin, and E.A. Roeloffs, Analysis of water level changes induced by fault creep at Parkfield, California, *J. Geophys. Res.*, *98*(B5), 8143-8152, 1993.

Rundle, J.W., Viscoelastic-gravitational deformation by a rectangular thrust fault in a layered Earth, *J. Geophys. Res.*, *87*(B2), 7787-7796, 1982.

Skempton, A.W., The pore-pressure coefficients A and B, *Geotechnique*, *4*, 143-147, 1954.

Terzaghi, K. Die Berechnung der Durchlassigkeitsziffer des toones aus dem Verlauf der Hydrodynamischen pannungserscheinungen, *Akad. Wiss. Wein Math. Naturwiss. K.*, *132*(3/4), 125-128, 1923. (reprinted in *From Theory to Practice in Soil Mechanics*, edited by L. Bjerrum, A Cassagrande, R. B. Peck, and A. W. Skempton, pp.133-146, John Wiley, New York, 1960.)

van der Kamp, G., and J. E. Gale, Theory of Earth tide and barometric effects in porous formation with compressible grains, *Water Resour. Res.*, *19*, 538-544, 1983.

Wang, H.F., Effects of deviatoric stress on undrained pore pressure response to fault slip, *J. Geophys. Res.*, *102*(B8), 17,943-17,950, 1997.

Wang, H.F., *Theory of Linear Poroelasticity with Applications to Geomechanics*, Princeton Press, Princeton, N.J., 2000.

S. Ge and S. C. Stover, Department of Geological Sciences, University of Colorado, Boulder, CO 80309-0399. (ges@spot.colorado.edu; shannon.stover@colorado.edu)

(Received September 17, 1999; revised March 29, 2000; accepted June 23, 2000.)